DOI:10.1021/jf900483t

JOURNAL OF AGRICULTURAL AND FOOD CHEMISTRY
ARTICLE

Native Lignin Structure of *Miscanthus x giganteus* and Its Changes during Acetic and Formic Acid Fractionation

Juan José Villaverde,[†,‡] Jiebing Li,*[,‡] Monica Ek,[‡] Pablo Ligero,[†] and Alberto de Vega[†]

[†]Department of Physical Chemistry and Chemical Engineering, University of A Coruña, 15071 A Coruña, Spain, and [‡]Department of Fiber and Polymer Technology, Royal Institute of Technology, KTH, SE-100 44 Stockholm, Sweden

Milled wood lignin (MWL) and acetic and formic acid lignin (AL and FL) from *Miscanthus x giganteus* bark were produced, respectively, before and after organosolv fractionations under optimal conditions, in terms of organic and hydrochloric acid concentrations, liquid/wood ratio, and reaction time. In order to study the *M. x giganteus* native lignin structure and its modifications during the fractionation process, the lignins were studied by two-dimensional heteronuclear single quantum coherence (2D-(HSQC)), ^{13}C- and ^{31}P nuclear magnetic resonance (NMR) spectroscopy, Fourier transform infrared (FTIR), size-exclusion chromatography (SEC) both before and after thioacidolysis, and elemental analysis. In addition, chemical composition analysis was performed on ash, Klason lignin, and carbohydrate content. The analyses demonstrated that *M. x giganteus* native lignin (MWL) is highly acylated at the C_γ of the lignin side chain (46%), possibly with *p*-coumarate and/or acetate groups. This is newsworthy since several earlier studies showed that acylation at the γ-carbon commonly occurs in C_3 and CAM grasses, whereas *M. x giganteus* is a C_4 grass. Furthermore, *M. x giganteus* showed a low S/G ratio (0.7) and a predominance of β-O-4′ linkages (up to 93% of all linkages). AL and FL lose part of these linkages during organosolv fractionation (up to 21 and 32%, respectively). The *p*-coumarate groups resist fractionation processes and are still present in high quantities in AL and FL. During the fractionation process, lignin is acetylated (acetic acid process) and condensed, with the G units condensing more than S units. *M. x giganteus* MWL contains a high content of carbohydrates (22.8%), suggesting that it is a lignin−carbohydrate complex (LCC). AL and FL showed low carbohydrate contents because of the breaking down of the LCC structures. AL and FL have high molecular weights and low polydispersities, and are high in phenolic content, qualities that make these suitable for different applications. These results suggest that refinement of *M. x giganteus* via organosolv processes could potentially turn this grass into a valuable source of both fiber and lignin.

KEYWORDS: *Miscanthus x giganteus*; perennial rhizomatous grass; lignin; 2D NMR; HSQC; ^{13}C NMR; ^{31}P NMR; SEC; FTIR; C9 formulas; thioacidolysis; carbohydrates; acetic acid; formic acid; organosolv; fractionation; LCC

INTRODUCTION

Vegetal biomass is one of the most logical natural sources for the sustainable production of organic chemicals. A model of sustainable development based on biomass will require the search for new renewable biomass sources, such as annual and perennial grasses. Among the grasses, those belonging to genus *Miscanthus* are important candidates to be plants of the future. This genus is originally from the tropics and subtropics, but different species are found throughout wide climatic regions in East Asia, Europe, and North America. Although they were originally introduced as ornamental plants from Japan in the 1930s, they have received more recent attention as potential energy crops because of their excellent productivity, fast growth, and low sensitivity to illnesses (*1*). *Miscanthus* grasses are tall, perennial, rhizomatous grasses, belonging to the Poaceae family, with C_4 photosynthesis (*1*). Because of their perennial nature and high productivity, these species are very attractive biomass sources. Among these grasses, *Miscanthus x giganteus* Greef & Deuter ex Hodkinson & Renvoize (*2*), a sterile hybrid horticultural genotype improperly referred to in some publications as *Miscanthus sinensis giganteus*, *Miscanthus sinensis*, *M. sinensis* var. 'Giganteus', *Miscanthus x ogiformis* Honda 'Giganteus', or *Miscanthus* 'Giganteus' has attracted the interest of EU authorities as a biomass source (*1*) for use in numerous applications (*3*) within the emerging field of biorefinery (*4*).

In recent decades, organosolv fractionation methods have attracted growing interest because they can be good environmental solutions for obtaining cellulose from different fiber

*To whom correspondence should be addressed. Tel: + 46 8 790 6165. Fax: + 46 8 790 6166. E-mail: jbing@kth.se.

 Published on Web 06/24/2009

sources. An important characteristic of these processes is that they result in few alterations in the fractionated materials; hence, they are considered in some contexts to be more valuable fractionation methods than ordinary pulping systems (*5*). Chemical upgrades in organosolv methods have opened the possibility of exploiting hemicelluloses and lignin from biomass, in addition to cellulose. Lignin is a polyphenolic amorphous material originating from the copolymerization of three phenylpropanoid monomers, i.e., coniferyl, sinapyl, and *p*-coumaryl alcohol, after the formation of various inter unit bonds, such as several types of ether (β-O-4′, α-O-4′, and 4-O-5′) and carbon−carbon linkages mediated by laccases and/or peroxidases (*6*, *7*). Because of its polyphenolic chemical structure, lignin can be used in manufacturing adhesives, epoxi- and phenolic-resins, and polyolefins as well as in a variety of nonspecific and novel applications. Despite this potential, only a small fraction of the lignin isolated from wood or other lignocellulosic biomass is commercially applied; instead, it is usually burned to generate energy. This situation is changing; however, as there is increasing support for true biorefineries that strive to take advantage of the complexity of biomass to maximize the production of high-value, low-volume and low-value, high-volume product fuels (*4*).

Deriving lignins from *M. x giganteus* using organosolv fractionation processes might be a good alternative to using grass as a fiber source, if lignin and lignin derivatives can be obtained with added value when compared to that of similar synthetic compounds derived from oil. Prior to making organosolv lignins from *M. x giganteus* available for various kinds of practical applications, the lignins must be characterized in terms of their purity, chemical structure, and properties.

It is well known that nuclear magnetic resonance (NMR) spectroscopy is one of the most widely used methods for the detailed structural characterization of lignin (*6*−*14*). Two-dimensional $^{1}H-^{13}C$ NMR (2D NMR) has been able to provide important structural information and has allowed for the resolution of otherwise overlapping resonances observed in either the ^{1}H or ^{13}C NMR spectra. It can also be used for semiquantitative analysis (*8*). Quantitative ^{13}C NMR itself is still a powerful tool for the analysis of the chemical structure of lignin. Moreover, detection of other nuclei, e.g., ^{31}P by ^{31}P NMR after derivatization with a ^{31}P containing reagent, has been widely used for the quantification of different types of hydroxyl groups in lignin (*9*). FTIR spectroscopy employs the mid-infrared region, and the band assignments have been intensely investigated (*11*, *12*, *15*). Some structural features such as aromatic structures, carbon−oxygen bonds, and carbonyl groups are clearly detectable. Analysis after thioacidolysis gives extremely valuable information about the content of β-aryl ether structures, with the exception of methyl aryl ethers (*16*). Size-exclusion chromatography (SEC) can be used to reveal information about the size of lignin or its fragments after various treatments. For example, SEC can be used in combination with thioacidolysis to observe condensation during fractionation processes, and this information can be complemented with gas chromatography flame ionization detection (GC-FID) to quantify the noncondensed β-O-4′ structures in samples after thioacidolysis (*16*−*18*).

In the present work, lignin from *M. x giganteus* bark in native form (MWL) and in fractionated form after acetic (AL) or formic (FL) acid processing was prepared. These various forms of lignin were then characterized using the techniques mentioned above in order to identify the lignin structure of *M. x giganteus* and the structure of modified products formed in the course of the fractionation process. C9 formulas for AL and FL were calculated, and the value of AL and FL for practical applications is discussed.

MATERIALS AND METHODS

Raw Material. *M. x giganteus* from an experimental plantation established near Santiago de Compostela (Spain) as part of the EU AIR *Miscanthus* Productivity Network was used in this study. Stems were harvested, manually stripped of leaves and bark, air-dried for two weeks, and ground to pass through a 1 cm sieve. Once in the laboratory, the moisture content of the ground substrate was allowed to equilibrate, and the samples were stored in hermetic polypropylene containers.

Acetic Acid and Formic Acid Fractionation. In the acetic acid process (Acetosolv), mixtures of ground *M. x giganteus* bark, water, and acetic acid (weight percentage with respect to cooking liquor = 90), were boiled in a 3 L glass reactor. Hydrochloric acid (weight percentage with respect to cooking liquor = 0.15) was added when boiling started, and the mixture was refluxed with stirring under atmospheric pressure for 55 min with a liquid/wood ratio of 12. For the formic acid fractionation, the process was similar (henceforth referred to as Formosolv to simplify nomenclature), with changes only in the type of organic acid (formic acid), the load of hydrochloric acid (weight percentage with respect to cooking liquor = 0.10), and the heating time (36 min). After heating, the pulp was filtered and treated four times with 85% acetic acid or 80% formic acid depending on the fractionation process (in w/v proportions of 0.4, 0.4, 0.2, and 0.2 with respect to the initial dry weight of *M. x giganteus*) and washed repeatedly with distilled water until neutrality was achieved. The process and reaction conditions used here have been optimized in previous works (*19*, *20*). After the fractionation process described above, the lignin was precipitated by treating given volumes of black liquor (**Figure 1**), with various volumes of water and then stirring. The precipitated solids were removed by centrifugation and repeatedly washed and centrifuged until the supernatant was neutral, after which the solids were freeze-dried. AL and FL were further purified by pentane extraction in a Soxhlet apparatus to remove extractives and with dioxane−water solution (9:1, v/v) to dissolve the lignin from carbohydrates and other impurities. The resultant solution was evaporated and freeze-dried.

Isolation of Milled Wood Lignin. Milled wood lignin (MWL) was extracted from finely milled wood meals that had previously been passed through a 20-mesh sieve and made free of extractives and materials soluble in hot water using previously described methods (*21*).

Acetylation of Lignins. Prior to SEC and NMR analysis of acetylated lignin (see below), lignin samples were acetylated as described earlier by applying a mixture of pyridine and acetic anhydride (1:1, v/v) and allowing the reaction to proceed overnight. After decomposition of the remaining acetic anhydride, the mixture was evaporated to dryness after subsequent additions of toluene and methanol (cf. ref (*17*)).

NMR Spectroscopy. On a Bruker Avance 400 MHz instrument, $^{13}C-^{1}H$ 2D heteronuclear single quantum coherence (HSQC) and quantitative ^{13}C NMR spectra were recorded after dissolving lignin in acetone-d_6−D_2O (3:1) solution at 25 °C using standard Bruker pulse programs (for a detail description, cf. ref (*8*)). In the aliphatic oxygenated region of HSQC spectra, the relative abundance of interunit linkages were estimated from $C_\alpha-H_\alpha$, and lignin acylation was estimated from the intensities of $C_\gamma-H_\gamma$ correlations in acylated and nonacylated side chains as previously described (*6*, *12*). In the aromatic region, the $C_{2,6}-H_{2,6}$ correlations from S units and the sum of C_2-H_2 and C_6-H_6 correlations from G units were used to estimate the S/G ratio (*6*, *12*). ^{31}P NMR spectra were acquired after derivatization with a ^{31}P containing reagent using a delay time of 10 s, and signal assignments were performed as previously described (cf. ref (*9*)).

Infrared Spectroscopy. FTIR spectra were obtained on a Perkin-Elmer Spectrum 2000 instrument by the attenuated total reflectance (ATR) technique. Spectra were recorded in the 4000−600 cm^{-1} range with 16 scans at a resolution of 4.0 cm^{-1} and an interval of 1.0 cm^{-1}.

Thioacidolysis. Thioacidolysis was performed in triplicate according to the methods reported in the literature (*16*). GC-FID analysis was performed after silylation, and SEC analysis was performed after acetylation using the same acetylation procedure as that described above. Quantification was conducted according to ref (*16*).

Gas Chromatography (GC). GC analysis was performed using an Rtx 5 column obtained from Restec Corporation (45 m, 0.32 μm I.D., 0.25 μm film thickness) with a temperature program of 180 °C/0 min to 270 °C/15 min and then to 300 °C/5 min at a rate of 4 °C/min. The injector

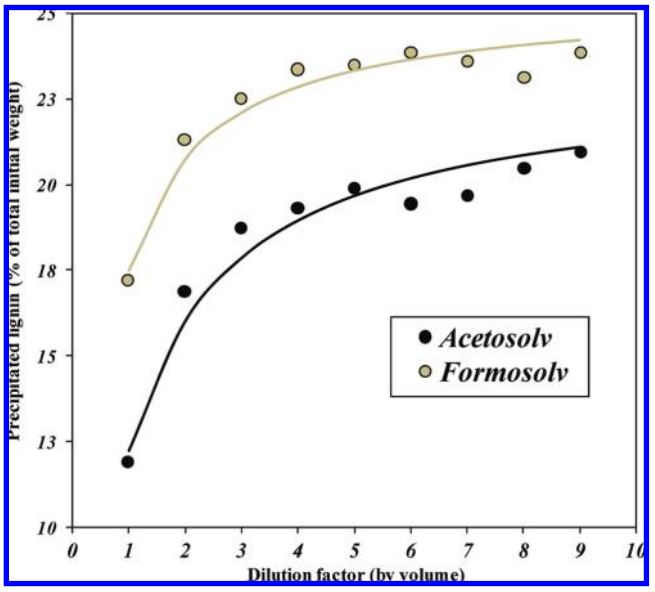

Figure 1. Dependence of lignin precipitation rate on dilution factor (ratio water/black liquor).

and detector temperatures were 250 and 280 °C, respectively. Helium was used as the carrier gas in a constant flow mode with split injection.

Size-Exclusion Chromatography (SEC). SEC runs were carried out on a system consisting of a series of three connected Ultrastyragel columns (100, 500, and 1000 Å) with a mobile phase of tetrahydrofuran (THF), at a flow rate of 0.8 mL/min, using a Waters 515 HPLC pump. Detection was performed using a Waters 2487 UV detector at 280 nm.

Composition Analysis. Acid-insoluble lignin (% Klason lignin), carbohydrate composition, and ash contents were determined in triplicate according to the TAPPI standards T 222 om-83, T 249 cm-85, and T 211 om-85.

Elemental Analysis. The C, H, and N contents of organosolv lignins were determined in triplicate by elemental analysis in a Carlo Erba EA 1108 automatic analyzer. The oxygen content was calculated from the difference between the sample weight and the C, H, and N contents. The methoxy group content was determined by subjecting the lignin to acid hydrolysis as previously described (*10*).

RESULTS AND DISCUSSION

Organosolv Fractionation. *M. x giganteus* bark is a good source of both pulp (fiber/cellulose) and lignin. Chemical analysis revealed its composition to be 26.1% Klason lignin, 73.3% holocellulose, 18.8% pentosans, and 0.4% ash on a dry weight basis. Organosolv fractionation is effective for pulp manufacturing. At optimal organic and hydrochloric acid concentrations, liquid/wood ratio, and reaction time, the efficiency of the Acetosolv process was very high, with a good pulp yield (58.8%), a kappa number suitable to start a bleaching process (17.0), and a high viscosity (1061 mL/g). For the Formosolv process, pulp yield (48.7%) and kappa number (23.0) were worse, but the viscosity (1197 mL/g) was higher, thereby making it suitable for bleaching. Furthermore, both pulps showed higher brightness (Acetosolv, 34.8% ISO; Formosolv, 30.6% ISO) than typical bleachable Kraft pulps (around 26% ISO).

After the fractionation process, lignins were obtained from the black liquors by dilution. In order to precipitate a greater quantity of lignin from the cooking liquors, different volumetric ratios of water to liquor were assayed. **Figure 1** shows the dependence of the lignin precipitation rates on the water−liquor ratio used. It was observed that the Formosolv fractionation method, using a water/liquor ratio of 6:1, produces a higher percentage of precipitate with respect to the dry weight of initial material (23.8%) than the Acetosolv process (19.4%). Most of the lignin was recovered since the original lignin content was 26.1% Klason lignin (see above), and it is therefore expected that a comparison between the fractionated lignins and native lignin would shed light on the structural changes during the organosolv fractionations.

Structural Characterization. Milled wood lignin (MWL) and the fractionated organosolv lignins (AL and FL) were characterized by different techniques. The main structural characteristics, such as the main interunit linkages of ether or C−C bonds (**Figure 2**), were revealed by the 2D HSQC spectra (**Figure 3**), and their proportions were estimated as described in Materials and Methods (**Table 1**). Here, the quantity data for AL and FL should be considered as semiquantitative because some errors might have resulted from lignin condensation and side chain elimination during the fractionation process.

Generally, the HSQC spectra could be divided into three regions of $^{13}C-^{1}H$ correlation corresponding to aliphatic (approximately δ_C/δ_H 0−50/0−2.5 ppm), oxygenated aliphatic (approximately δ_C/δ_H 50−100/2.5−6.5 ppm), and aromatic (approximately δ_C/δ_H 100−160/5.5−9 ppm) regions. Signals in the aliphatic region are usually considered to originate from impurities, such as those from extractives like fatty acids (*11*), and the signals of acetyl correlations are also included in this region (alcoholic acetates δ_C/δ_H 21.2/2.02 ppm (*12*) and phenolic acetates δ_C/δ_H 20.1/2.49 ppm (*12*)), which might be useful to estimate the phenolic and alcoholic hydroxyls after acetylation. This first region is less valuable in this work, however, since we used quantitative ^{13}C NMR after acetylation and ^{31}P NMR after derivatization with the ^{31}P reagent, which are more accurate techniques than HSQC (*9*, *14*) to estimate the phenolic and alcoholic hydroxyls (**Table 2**). The main lignin cross-signals used are from the oxygenated aliphatic and aromatic regions and were assigned by comparison with the literature (refs (*6*, *7*, *11*, *12* and *22*), and references therein) (**Table 3**). Also, signals at δ_C/δ_H 102.9/4.38 ppm indicate the anomeric C_1-H_1 correlations of xylan (*12*).

In addition, acetylation was performed for isolated lignins, and the comparison of the HSQC spectra before and after acetylation could further assist in the assignment of signals. ^{13}C NMR was used to quantify the extent of acetylation in the structure of lignin, which supplies the information about the acylation progress throughout the fractionation processes and during the acetylation reaction performed on the fractionated lignins (**Table 2**). ^{31}P NMR spectra were also obtained and used for the quantification of carboxyl groups as well as of various types of hydroxyls (**Table 2**).

Furthermore, various functional groups and structural fragments were characterized by FTIR (**Figure 4**). The infrared spectra generally showed a typical band between 1645 and 1760 cm^{-1} corresponding to the stretching of conjugated and nonconjugated carbonyls with the aromatic ring, although the band could also be due to carboxyl groups or bands of aliphatic acetates. The FTIR spectrum had typical lignin patterns, including bands of aromatic ring vibrations at 1600 cm^{-1} and 1520−1400 cm^{-1}. Other bands were due to aromatic ring breathing of S (1330 cm^{-1}) and G units (1263 cm^{-1} shoulder), aromatic in-plane bending in S (1123 cm^{-1}) and G units (1034 cm^{-1}), and out-of-plane C−H bending of G (916 cm^{-1}) and S units (835 cm^{-1}). Finally, if the sample contained carbohydrates, the FTIR spectrum of lignin also included carbohydrate bands around 1000 cm^{-1} (*15*).

SEC analysis on the acetylated lignin samples, before and after thioacidolysis, was used to evaluate the molecular size and distribution of the lignin samples and their fragments after the

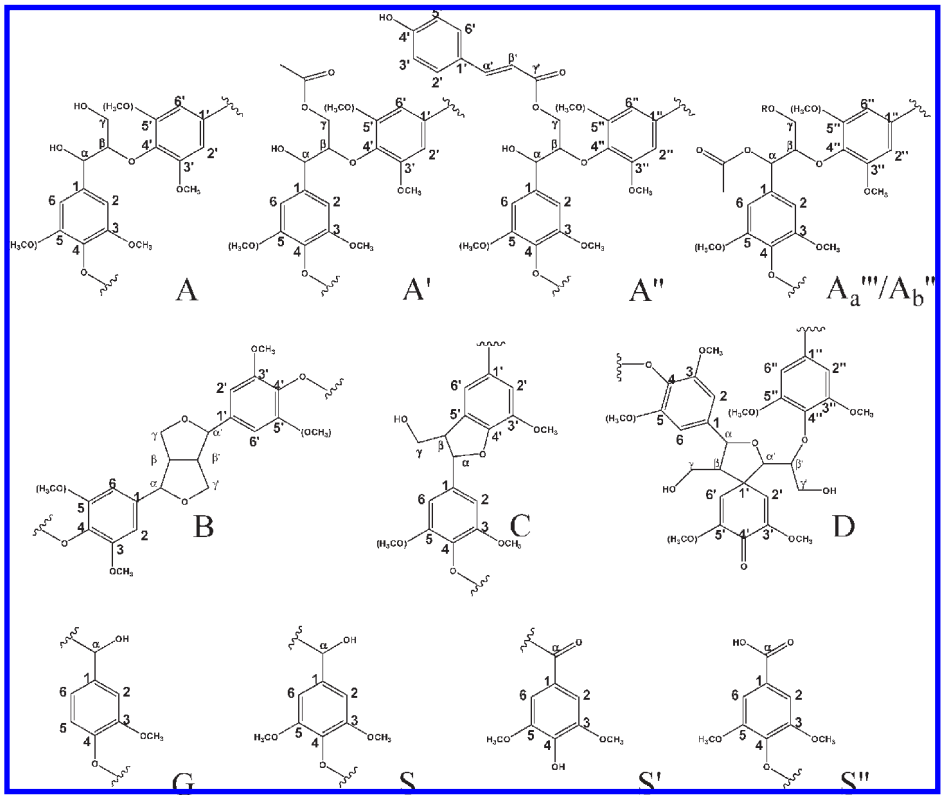

Figure 2. Main structures identified in *M. x giganteus* lignin: (**A**) β-O-4′ aryl ether linkages with a free −OH at the γ-carbon; (**A′**) β-O-4′ aryl ether linkages with acetylated −OH at γ-carbon; (**A″**) β-O-4′ aryl ether linkages with *p*-coumaroylated −OH at γ-carbon; (**A$_a$‴**) β-O-4′ aryl ether linkages with α-acylated substructure, which is especially abundant in the in vitro acetylated lignins (R=acetyl); (**A$_b$‴**) β-O-4′ aryl ether linkages with α-acylated substructure, which is especially abundant in the in vitro acetylated lignins (R = *p*-coumaroyl); (**B**) resinol structures formed by $\beta-\beta'$, α-O-γ', and γ-O-α' linkages; (**C**) phenylcoumarane structures formed by β-5′ and α-O-4′ linkages; (**D**) spirodienone structures formed by β-1′, α-O-α' linkages; (**G**) guaiacyl unit; (**S**) syringyl unit and (**S′** and **S″**) oxidized syringyl units with a C_α ketone or a C_α carboxyl group.

complete cleavage of all β-O-4′ linkages (**Figure 5** and **Table 4**). After thioacidolysis, GC-FID analysis showed the quantification of noncondensed β-O-4′ structures as well as the ratio of S/G lignin units (**Table 1**).

Finally, the ash, Klason lignin, and carbohydrate content and compositions were determined (**Table 5**). Also C, H, N, O, and methoxy contents were determined and a combined C9 formula for AL or FL was calculated, demonstrating the overall structure and structural differences in AL and FL (**Table 2**).

Native *M. x giganteus* Lignin (MWL). The oxygenated aliphatic region of the 2D HSQC spectra (**Figure 3A**) clearly showed the methoxy substituents (δ_C/δ_H 56.5/3.73). Side-chain signals from different β-O-4′ linkages could also be observed, implying that various β-O-4′ structures (**Figure 2**) from different aromatic rings in the native lignin were present. A characteristic of *M. x giganteus* MWL is a high proportion of β-O-4′ ether linkages of up to 93% of all linkages. This is in accordance with previously published data for highly acylated lignins from other nonwoody plants such as kenaf, sisal, abaca, and curaua (*6*, *7*). Lignin contains a very low proportion of condensed linkages such as spirodienone (β-1′) (detected in a quantity lower than 0.5%), phenylcoumaran (β-5′) and resinol ($\beta-\beta'$) (**Table 1**) which could be interpreted as follows:

(1) Spirodienone (β-1′, α-O-α', linkages) substructures (**D**): $C_\alpha-H_\alpha$ (δ_C/δ_H 82.5/5.11 ppm), $C_{\alpha'}-H_{\alpha'}$ (δ_C/δ_H 85.4/4.91 ppm), and $C_\beta-H_\beta$ (δ_C/δ_H 54.9/3.04 ppm) (*6*, *7*). These substructures were found as well with small signals in lignins of C_3 and CAM photosynthesis grasses (*6*).

(2) Resinol ($\beta-\beta'$ linkages) substructure (**B**): $C_\alpha-H_\alpha$, $C_\beta-H_\beta$, and $C_\gamma-H_\gamma$ (at δ_C/δ_H 86.4/4.67, 54.9/3.30, and 72.5/4.19 (and a very weak 72.5/3.83) respectively) (*6*, *7*). Resinols were also observed in kenaf and hemp lignins with strong signals (*6*, *7*) and in sisal lignin with weak signals (*6*, *7*).

(3) Phenylcoumaran (β-5′ linkages) substructures (**C**): $C_\alpha-H_\alpha$ (δ_C/δ_H 88.3/5.48 ppm) (*6*, *7*) and $C_\beta-H_\beta$ (δ_C/δ_H 54.7/3.46 ppm) (*6*, *7*). The presence of these substructures is directly related to the existence of guaiacyl units in lignins and was also previously observed in the native lignin of some nonwoody angiosperms (*6*, *7*).

It is believed that the high acylation at C_γ (see below) could be the reason for the low abundance of the double tetrahydrofuran ring from resinol, which requires free hydroxyls in C_γ to be formed (*23*). Moreover, it was possible, on the basis of HSQC analysis, to estimate that 46% of γ-carbons are acylated (**Table 1**).

The aromatic region in the 2D HSQC spectra (**Figure 3B**) showed normal syringyl (S)- and guaiacyl (G)-rings in lignin. The former showed a strong signal for the $C_{2,6}-H_{2,6}$ correlation at δ_C/δ_H 104.8/6.71 ppm (*6*, *7*, *11*, *12*, *22*), and the latter showed different correlations for C_2-H_2, C_5-H_5, and C_6-H_6 (at δ_C/δ_H 111.3/6.95, 115.5/6.71−116.7/6.92, and 120.4/6.81 ppm, respectively (*6*,*7*,*11*,*12*,*22*)). From the analysis of this region, it could be concluded that lignin contains C_α-oxidized structures since the signals corresponding to $C_{2,6}-H_{2,6}$ correlations in C_α-oxidized S units (**S′** and **S″**) were observed at δ_C/δ_H 107.4/7.32 and 107.8/7.17, respectively (*6*, *7*, *11*, *12*, *22*).

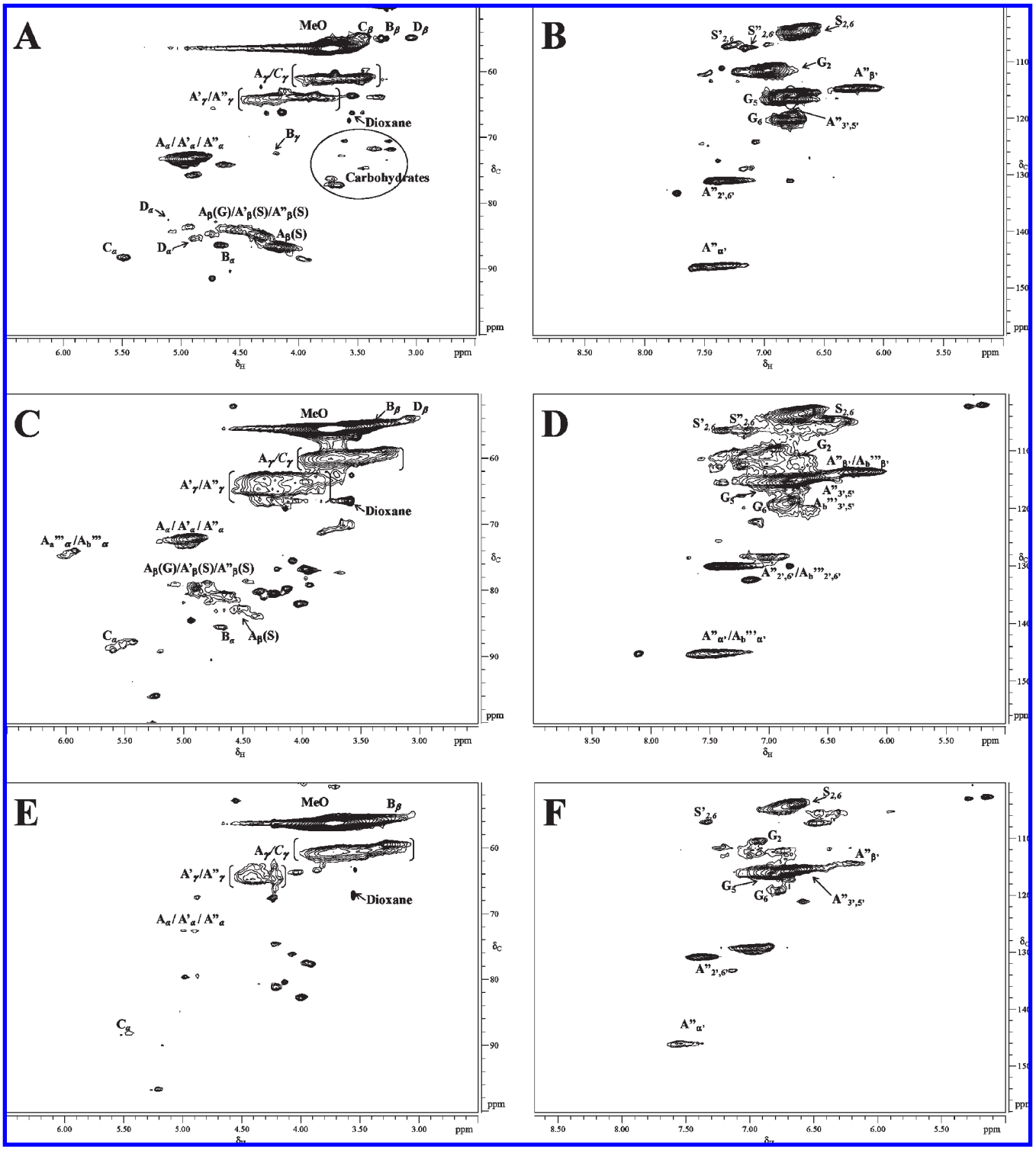

Figure 3. Oxygenated aliphatic (left column) and aromatic regions (right column) in the HSQC 2D NMR spectra: δ_C/δ_H 50−100/2.5−6.5 ppm and δ_C/δ_H 100−160/5.0−8.5 ppm, respectively. (**A** and **B**) milled wood lignin (MWL); (**C** and **D**) Acetosolv lignin (AL); (**E** and **F**) Formosolv lignin (FL). Symbols are taken from **Figure 2**.

The signal assignments were further confirmed by performing 2D HSQC NMR analysis on in vitro acetylated MWL, where the major difference from the original MWL found was in δ_C and δ_H corresponding to correlations $C_\beta-H_\beta$ (δ_C/δ_H 81.1/4.63 ppm) and $C_\alpha-H_\alpha$ (δ_C/δ_H 75.0/5.94 ppm) in β-O-4′ substructures (*12*) because of acetylation at the C_α or C_γ position. The resinol substructures did not have free hydroxyls in their side chains, and therefore, cross-signals were barely affected after its acetylation ($C_\alpha-H_\alpha$, $C_\beta-H_\beta$, and $C_\gamma-H_\gamma$ correlations with δ_C/δ_H 86.2/4.66, 54.8/3.23, and 72.3/3.82 and 4.17 ppm, respectively (*12*)).

In the literature, abaca and curaua native lignins have been reported to be naturally esterified by *p*-coumaric acid to the lignin polymer (*6*, *13*, *23*−*25*). In *M. x giganteus* MWL, *p*-coumarate structures were in fact observed by very prominent signals. Aromatic ring cross-signals corresponding to correlations $C_{2',6'}-H_{2',6'}$ and $C_{3',5'}-H_{3',5'}$ were observed at δ_C/δ_H 131.1/7.35 and 116.8/6.80 ppm (*6*, *7*), respectively. In addition, signals of

unsaturated $C_{\alpha'}-H_{\alpha'}$ and $C_{\beta'}-H_{\beta'}$ of the *p*-coumarate unit in structure **A″** of **Figure 2** were also observed at δ_C/δ_H 146.3/7.41 and 114.6/6.18 ppm, respectively (*6*, *7*). Acetylated lignin units in native lignin have also been widely reported in several plants (*26*−*28*) arising from the polymerization of preacetylated monomers (*27*, *29*). **Figure 3A** shows that in *M. x giganteus* MWL, the correlation signals of naturally γ-acylated β-O-4′ (**A′** and **A″**) $C_\alpha-H_\alpha$ (δ_C/δ_H 73.1/4.88 ppm) (*6*, *7*) could be observed, although they overlapped with the β-O-4′ correlation ($C_\alpha-H_\alpha$) signal (**A**) and also with γ-acylated β-O-4′ $C_\beta-H_\beta$ (δ_C/δ_H 84.1−86.7/4.17−4.52 ppm) (*6*, *7*). It was concluded that *M. x giganteus* native lignin (MWL) is highly acylated at C_γ, possibly with *p*-coumarate and/or acetate groups. After in vitro acetylation, the $C_{3',5'}-H_{3',5'}$ correlation signal at the *p*-coumarate structures was noticeably shifted to δ_C/δ_H123.2/7.08 ppm, indicating that there were free phenolic groups at C4′ of the *p*-coumarate before acetylation, which indirectly supports the ester linkages of *p*-coumarate structures to the lignin side chain as shown in structure **A″** (**Figure 2**). In order to obtain additional information about the exact nature of the acyl groups as well as the moiety (S- or G-units) to which these groups are attached, HMBC analysis (*11*, *12*) or DFRC degradation analysis (*6*) would be needed.

The composition analysis revealed that *M. x giganteus* native lignin contains substantial amounts of carbohydrates (22.8%), mainly pentoses (**Table 5**). The HSQC spectra also revealed the presence of carbohydrates (**Figure 3A**). This was further confirmed by FTIR analysis, which revealed carbohydrate bands around 1000 cm^{-1}. Therefore, the isolated MWL is in fact a lignin−carbohydrate complex (LCC) rather than pure lignin. There were, as could be expected, chemical linkages present between the lignin and carbohydrates perhaps in a form of short chain polysaccharides. This is in agreement with the fact that grass plants have a large percentage of pentosans linked to lignin by ether and ester bonds.

Table 1. Estimated Quantities of the Inter-Unit Linkages (% of Side Chains Involved in Substructures **A**−**D**), Extent of Acylation (% of γ-Acylation), and S/G Ratios by HSQC as well as S/G Ratios by Thioacidolysis in Milled Wood Lignin (MWL), Acetosolv Lignin (AL), and Formosolv Lignin (FL)

	interunit linkage					S/G ratio	
sample	β-O-4′	β-1′	β-5′	β-β′	% of γ-acylation	thioacidolysis	HSQC
MWL	93	trace[a]	3	4	46	0.7	0.7
AL	73	trace[a]	23	4	55	1.8	1.3
FL	63	0	37	trace[a]	31	2.0	0.8

[a] Percentage lower than 0.5%.

Table 2. Functional Groups Quantified by NMR and Elemental Analysis Results for *M. x giganteus* Milled Wood Lignin (MWL), Acetosolv Lignin (AL), and Formosolv Lignin (FL)

		functional group content by ^{31}P NMR (mmol/g)									acetylated groups (OCOR) per C_9 unit by ^{13}C NMR	
				OH^{Ph}								
sample	complex C9 formulas	COOH	OH^{Al}	S	G	H	MeO- by GC (mmol/g)	simple C_9 formulas	molecular weight (g/mol)	proteins (%)	after isolation	after acetylation
MWL		0.18	5.54	0.14	0.38	0.32					0.28	1.73
AL	$C_9H_{6.87}O_{2.19}(OCH_3)_{1.01}(COOH)_{0.04}(OH^{Ph})_{0.43}(OH^{Al})_{0.22}$	0.21	1.11	0.79	0.78	0.62	5.21	$C_9H_{9.48}O_{3.52}$	173.97	1.00	0.37	0.50
FL	$C_9H_{7.04}O_{2.64}(OCH_3)_{0.65}(COOH)_{0.02}(OH^{Ph})_{0.41}(OH^{Al})_{0.15}$	0.09	0.79	0.73	0.68	0.51	3.47	$C_9H_{8.91}O_{3.62}$	175.00	1.00	0.07	0.25

Table 3. Assignment of Main Lignin $^{13}C-^{1}H$ Cross-Signals in the HSQC Spectra of *M. x giganteus* MWL

δ_C/δ_H (ppm)	assignment
54.7/3.46	$C_\beta-H_\beta$ in phenylcoumaran substructures (**C**)
54.9/3.04	$C_\beta-H_\beta$ in β-1′ (spirodienone) substructures (**D**)
54.9/3.30	$C_\beta-H_\beta$ in $\beta-\beta'$ (resinol) substructures (**B**)
60.9/3.35−4.03	$C_\gamma-H_\gamma$ in β-O-4′ and phenylcoumaran substructures (**A** and **C**)
63.8/3.71−4.43	$C_\gamma-H_\gamma$ in γ-acylated β-O-4′ substructures (**A′** and **A″**)
72.5/4.19 (and 72.5/3.83[a])	$C_\gamma-H_\gamma$ in $\beta-\beta'$ (resinol) substructures (**B**)
73.1/4.88	$C_\alpha-H_\alpha$ in β-O-4′ substructures (**A**, **A′** and **A″**)
82.5/5.11	$C_\alpha-H_\alpha$ in β-1′(spirodienone) substructures (**D**)
84.1/4.52	$C_\beta-H_\beta$ in γ-acylated β-O-4′ substructures linked to S-type units (**A′** and **A″**) and $C_\beta-H_\beta$ in β-O-4′ structures linked to a G-type unit (**A**)
86.4/4.67	$C_\alpha-H_\alpha$ in $\beta-\beta'$ (resinol) substructures (**B**)
85.4/4.91	$C_{\alpha'}-H_{\alpha'}$ in β-1′(spirodienone) substructures (**D**)
86.7/4.17[b]	$C_\beta-H_\beta$ in β-O-4′ substructures linked to a S-type units (**A**)
88.3/5.48	$C_\alpha-H_\alpha$ in phenylcoumaran substructures (**C**)
104.8/6.71	$C_{2,6}-H_{2,6}$ in syringyl units (**S**)
107.4/7.32	$C_{2,6}-H_{2,6}$ in oxidized (C_α=O) syringyl units (**S-′**)
107.8/7.17	$C_{2,6}-H_{2,6}$ in oxidized (C_αOOH) syringyl units (**S″**)
111.3/6.95	C_2-H_2 in guaiacyl units (**G**)
114.6/6.18	$C_{\beta'}-H_{\beta'}$ in *p*-coumaroylated substructures (**A″**)
115.5/6.71 and 116.7/6.92	C_5-H_5 in guaiacyl units (**G**)
116.8/6.80	$C_{3',5'}-H_{3',5'}$ in *p*-coumaroylated substructures (**A″**)
120.4/6.81	C_6-H_6 in guaiacyl units (**G**)
131.1/7.35	$C_{2',6'}-H_{2',6'}$ in *p*-coumaroylated substructures (**A″**)
146.3/7.41	$C_{\alpha'}-H_{\alpha'}$ in *p*-coumaroylated substructures (**A″**)

[a] Too weak to be seen directly in **Figure 3** but observable after increasing the intensity of 2D-NMR. [b] Includes $C_\beta-H_\beta$ signals, at δ_C/δ_H 86.4/4.11 and 87.3/4.01 ppm, corresponding, respectively, to the *erythro* and *threo* forms of side chains.

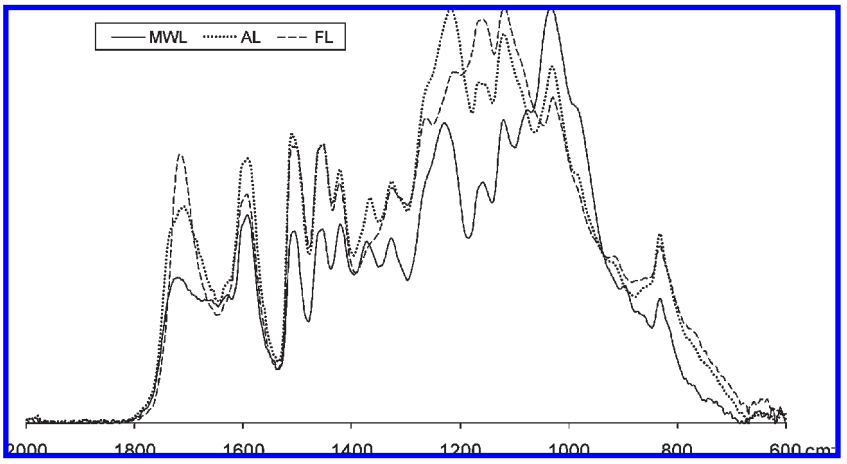

Figure 4. FTIR spectra (2000−600 cm^{-1}) of milled wood lignin (MWL), Acetosolv lignin (AL), and Formosolv lignin (FL).

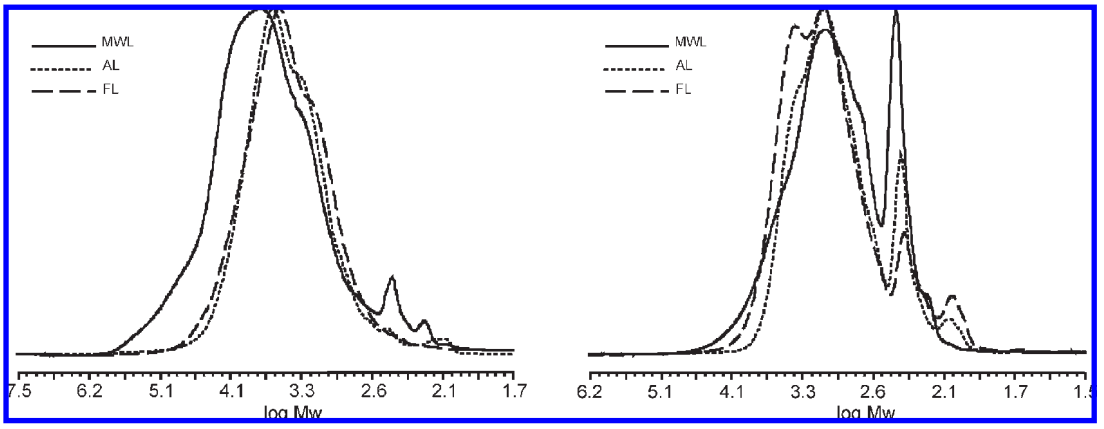

Figure 5. SEC of milled wood lignin (MWL), Acetosolv lignin (AL), and Formosolv lignin (FL) before (**left**) and after (**right**) thioacidolysis.

Table 4. Weight Average (M_w), Number Average (M_n) Molecular Weights, Molecular Weight at Maximum Peak (M_p), and Polydispersity (D) of *M. x giganteus* Milled Wood Lignin (MWL), Acetosolv Lignin (AL), and Formosolv Lignin (FL)

sample	M_w (Da)	M_n (Da)	M_p (Da)	D
MWL	31742	2681	10125	11.84
AL	6024	1444	3869	4.17
FL	6656	2122	4233	3.14

Lignin Structural Modification during Organosolv Fractionation. Substantial structural changes were noticed when comparing the 2D NMR spectra of AL and FL with MWL, where the presence of a greater number of signals and broader signals implied more complicated lignin structures after the fractionation processes. The most important changes were observed at the β-O-4′ correlation ($C_\alpha-H_\alpha$ and $C_\beta-H_\beta$) signals. In comparison to MWL (**Figure 3A**), the corresponding intensities in AL (**Figure 3C**) were lower and in FL (**Figure 3E**) were much lower. As a result of the substantial β-O-4′ cleavages, the lignin molecular weight decreased in AL (Mp 3869 Da) and FL (Mp 4233 Da) (compared to MWL of Mp 10125 Da) (**Table 4**) as shown in the SEC analysis comparison (left curves of **Figure 5**).

After thioacidolysis, which broke down all β-O-4′ bonds, the molecular weight of the lignin fragments was still high for both AL and FL. This suggested some extent of condensation during the Acetosolv and Formosolv processes, as could be seen when comparing the SEC curve after thioacidolysis of MWL with AL and FL (right curves in **Figure 5**). The fragments from MWL were lower in molecular weight because of fewer condensed structures. Furthermore, the analysis of the monomeric thioacidolysis products showed S/G ratios of 1.8 and 2.0 for AL and FL, respectively, with barely detectable amounts of *p*-coumaryl rings (H) in both cases. On the contrary, MWL presented an S/G ratio of 0.7, revealing that condensation takes place preferably at G units, i.e., through the free C_5 or C_6 position. For any H units present, condensation will be greater since they should be more reactive toward the condensation reaction than the G units. Therefore, after these two organosolv processes, fewer intact recalcitrant lignin structures (e.g., G units) survived when compared to those present in MWL. For comparison, the S/G ratio was also calculated from the HSQC spectra (**Table 1**). It could be seen that the data obtained are very close to the results from the thioacidolysis analysis. However, the latter is considered more accurate because of the overlapping signals at the HSQC spectra.

However, AL presented an infrared spectrum more similar to MWL than FL (but very similar between AL and FL), with the biggest difference being in the band of carbohydrates, which is more intensive in MWL. In accordance with the infrared spectra, the carbohydrate analysis of AL and FL (**Table 5**) showed only negligible amounts of carbohydrates (1.4−2.2%) before the purification with dioxane/water solutions. The organosolv lignins monosaccharide distribution was still high in pentoses (77.9−79.1% of pentoses and only 20.8−22.1% hexoses). The ratio of xylose/pentoses, however, was lower than that in MWL, implying that a high percentage of xylose is removed during fractionation.

As learned from the HSQC NMR experiments after the in vitro acetylation mentioned above, the two signals δ_C/δ_H 74.4/5.98 and 63.8/3.73−4.56 ppm (**Figure 3C**) represent acetylations at C_α and

Table 5. Compositions and Relative Carbohydrate Compositions of Milled Wood Lignin (MWL), Acetosolv Lignin (AL), and Formosolv Lignin (FL)

					pentoses		hexoses		
	sample	Klason lignin (%)	ash (%)	total carbohydrates (%)	arabinose (%)	xylose (%)	mannose (%)	galactose (%)	glucose (%)
MWL		61.3	0.3	22.8	7.5	78.4	0.8	3.1	10.2
AL	without purification	90.4	0.0	1.4	41.3	36.6	1.4	2.0	18.7
	with purification	91.1	0.0	1.2	43.5	36.7	1.5	2.0	16.3
FL	without purification	92.1	0.1	2.2	38.4	40.7	1.7	1.7	17.4
	with purification	92.8	0.0	1.9	42.6	41.0	1.4	1.2	13.8

C_γ, respectively, in the β-O-4′ structure. In AL, more acetylated $C_\alpha-H_\alpha$ was observed than in MWL. Slightly more acetylation of $C_\gamma-H_\gamma$ was observed, implying the simultaneous hydrolysis of native esters and that acetylation (esterification) was taking place under acidic conditions during fractionation. In FL, the acylation degree of the γ-carbon (possibly with *p*-coumarate and/or acetate groups) remained in lower amounts than that in the AL. This is reasonable since formic acid is a stronger acid than acetic acid and thus caused more severe hydrolysis. Additionally, there was no acetylation involved in the formic acid fractionation to compensate for reacetylation.

Contrary to the Acetosolv treatment that generated a broadening of the aromatic signals (for S and G units), the Formosolv treatment narrowed the signals. It was noticed that the spirodienone signal disappeared after the Formosolv fractionation process and that only the $C_\beta-H_\beta$ (δ_C/δ_H 54.9/3.04 ppm) signal (*6*, *7*) for spirodienone and the $C_\alpha-H_\alpha$ (δ_C/δ_H 88.3/5.48 ppm) signal (*6*, *7*) for phenylcoumaran still appeared in AL. After the fractionation process, the signals for resinol either disappeared or overlapped. Because of the fact that formic acid is a stronger acid, the β-O-4′ signals almost completely disappeared after the Formosolv process, whereas the same resonances did not show substantial changes after the Acetosolv treatment (see above). The C_α-oxidized structures seem very stable during fractionation since the signals corresponding to the $C_{2,6}-H_{2,6}$ correlations in the C_α-oxidized S units (**S′** and **S″**) (107.4/7.32 and 107.8/7.17, respectively (*6*, *7*, *11*, *12*, *22*)) could still be observed in AL and FL (although in the latter, only **S′** is observed).

It could be concluded that the chemical modifications taking place during the acid organosolv fractionation are β-O-4′ cleavage, lignin condensation under acidic conditions, hydrolysis of LCC structures and of the native ester structures, and esterification of the hydroxyl groups by organic acids.

Fractionated Organosolv Lignins. AL and FL are more pure lignins than MWL, as could be seen from their ash (~0%), Klason lignin content (>90%), and carbohydrate content (1−2%) (**Table 5**). This shows that they are ideal lignins to use industrially without any further purification other than the neutralization with water already performed during preparation.

However, the apparent weight average molecular weight (M_w) and apparent number average molecular weight (M_n) of AL and FL are around 6000 and 1000−2000 Da, respectively (**Table 4**), showing higher molecular weights and lower polydispersities (*D*) (3.14−4.17) than Kraft lignins or lignosulphonates (*17*).

Information about phenolic and alcoholic hydroxyls in MWL and organosolv lignins obtained from ^{13}C NMR and ^{31}P NMR analyses is included in **Table 2**. Calculations from ^{13}C NMR data for AL and FL showed that free hydroxyl groups accounted for 26% and 72%, respectively, of all groups susceptible to undergo acetylation and are available for derivatization reactions. This percentage is the amount of the original hydroxyls plus the hydroxyls hydrolyzed from the ester groups minus those being consumed in the generation of new ester structures during acidic fractionation. This corresponded to 12% fewer in AL and 58% fewer in FL free hydroxyl groups compared to those in MWL. ^{31}P NMR could further divide the total hydroxyl group content into aliphatic and various types of phenolic groups and allow an analysis of the quantity of COOH groups. The analysis showed that the organosolv processes lead to a large reduction in the number of aliphatic hydroxyl groups and a large increase in phenolic hydroxyl groups in relation to those in *M. x giganteus* native lignin. In addition, as the reactivity of lignin is essentially influenced by the number of phenolic groups (AL contains 2.19 mmol/g, and FL contains 1.92 mmol/g) by ring activation through the formation of highly nucleophilic quinonemethide intermediates, these lignins would be expected to react well with nucleophilic agents.

After elemental analysis, the simple C9 formula as well as the molecular weights for an average C9 lignin unit and the percentage of proteins in the recovered lignins were obtained for AL and FL. When these values were further combined with the quantities of the different functional groups mentioned above, complex C9 formulas could be calculated (**Table 2**). From this table, it can be seen that AL and FL might have different structures since AL has more hydroxyls groups than FL. The low carboxyl content of both lignins (<1%, in comparison to typical values of >6% for Kraft lignins) suggests that they underwent lower alteration during the organosolv fractionation processes than the Kraft lignins. This result is consistent with the results from the HSQC, FTIR, and SEC analyses mentioned above. Finally, the relatively low methoxy content (3.47−5.21 mmol/g) implies that these lignins have sufficient free ortho positions and therefore must be reactive and usable for a variety of applications such as in the manufacturing of phenol−lignin−formaldehyde resins.

It can be concluded from this study that *M. x giganteus* native lignin is acylated probably at the γ-carbon of the lignin side chain by *p*-coumarate and/or acetate groups. This important acylation results in a low abundance of $\beta-\beta'$ resinol linkages. It is remarkable that almost all earlier observations of native γ-carbon acylation were reported in C_3 and CAM grasses, whereas *M. x giganteus* is a C_4 grass. These esters persist after organosolv fractionation, and in AL, C_α is further acetylated during fractionation. Organosolv processes led to a large reduction in the number of aliphatic hydroxyl groups and a large increase in phenolic hydroxyl groups. AL and FL are similar and possess a very low carbohydrate content, implying that the organosolv fractionation processes broke down LCC structures and removed xylose from the native lignin in large quantities. The two organosolv lignins possess a high molecular weight and low polydispersity, and have fewer G units than MWL because of the lignin condensation during the fractionation processes studied. An important reactivity of AL and FL from *M. x giganteus* with nucleophilic agents can be presumed because of the presence of substantial amounts of free phenolic groups.

ACKNOWLEDGMENT

We thank Dr. David Ibarra at KTH for help with the interpretation of HSQC spectra and Dr. D. Manuel Bao Iglesias, from the University of Santiago de Compostela, for kindly supplying the *M. x giganteus* samples.

LITERATURE CITED

(1) Lewandowski, I.; Clifton-Brown, J. C.; Scurlock, J. M. O.; Huisman, W. Miscanthus: European experience with a novel energy crop. *Biomass Bioenergy* **2000**, *19*, 209–227.

(2) Hodkinson, T. R.; Renvoize, S. Nomenclature of *Miscanthus x giganteus* (Poaceae). *Kew Bull*. **2001**, *56*, 759–760.

(3) Villaverde, J. J.; Domingues, R. M. A.; Freire, C. S. R.; Silvestre, A. J. D.; Pascoal Neto, C.; Ligero, P.; Vega, A. *Miscanthus x giganteus* extractives: A source of valuable phenolic compounds and sterols. *J. Agric. Food Chem*. **2009**, *57*, 3626–3631.

(4) Fernando, S.; Adhikari, S.; Chandrapal, C; Murali, N. Biorefineries: current status, challenges, and future direction. *Energy Fuels* **2006**, *20*, 1727–1737.

(5) Vila, C.; Santos, V.; Parajó, J. C. Optimization of beech wood pulping in catalyzed acetic acid media. *Can. J. Chem. Eng*. **2000**, *78*, 964–973.

(6) del Río, J. C.; Rencoret, J.; Marques, G.; Gutiérrez, A.; Ibarra, D.; Santos, J. I.; Jiménez-Barbero, J.; Zhang, L.; Martínez, A. T. Highly acylated (acetylated and/or *p*-coumaroylated) native lignins from diverse herbaceous plants. *J. Agric. Food Chem*. **2008**, *56*, 9525–9534.

(7) Martínez, A. T.; Rencoret, J.; Marques, G.; Gutiérrez, A.; Ibarra, D.; Jiménez-Barbero, J.; del Río, J. C. Monolignol acylation and lignin structure in some nonwoody plants: A 2D-NMR study. *Phytochemisty* **2008**, *69*, 2831–2843.

(8) Zhang, L. M.; Gellerstedt, G. Quantitative 2D HSQC NMR determination of polymer structures by selecting suitable internal standard references. *Magn. Reson. Chem*. **2007**, *45*, 37–45.

(9) Granata, A.; Argyropoulos, D. S. 2-Chloro-4,4,5,5-tetramethyl-1,3,2-dioxaphospholane, a reagent for the accurate determination of the uncondensed and condensed phenolic moieties in lignins. *J. Agric. Food Chem*. **1995**, *43*, 1538–1544.

(10) Ligero, P.; Villaverde, J. J.; Vega, A.; Bao, M. Delignification of *Eucalyptus globulus* saplings in two organosolv systems (formic and acetic acid). Preliminary analysis of dissolved lignins. *Ind. Crops Prod*. **2008**, *27*, 110–117.

(11) Ibarra, D.; Chávez, M. I.; Rencoret, J.; del Río, J. C.; Gutiérrez, A.; Romero, J.; Camarero, S.; Martínez, M. J.; Jiménez-Barbero, J.; Martínez, A. T. Structural modification of eucalypt pulp lignin in a totally chlorine-free bleaching sequence including a laccase-mediator stage. *Holzforschung* **2007**, *61*, 634–646.

(12) Ibarra, D.; Chávez, M. I.; Rencoret, J.; del Río, J. C.; Gutiérrez, A.; Romero, J.; Camarero, S.; Martínez, M. J.; Jiménez-Barbero, J.; Martínez, A. T. Lignin modification during *Eucalyptus globulus* kraft pulping followed by totally chlorine-free bleaching: a two-dimensional nuclear magnetic resonance, fourier transform infrared, and pyrolysis-gas chromatography/mass spectrometry study. *J. Agric. Food Chem*. **2007**, *55*, 3477–3490.

(13) Holtman, K. H.; Chang, H. M.; Jameel, H.; Kaddla, J. F. Quantitative ^{13}C NMR characterization of milled wood lignins isolated by different milling techniques. *J. Wood Chem. Technol*. **2006**, *26*, 21–34.

(14) Robert, D. Carbon-13 Nuclear Magnetic Resonance Spectrometry. In *Methods in Lignin Chemistry*; Lin, S. Y., Dence, C. W., Eds.; Springer-Verlag: Berlin, Germany, 1992; pp 250−273.

(15) Faix, O. Classification of lignins from different botanical origins by FT-IR Spectroscopy. *Holzforschung* **1991**, *45*, 21–27.

(16) Rolando, C.; Monties, B.; Lapierre, C. Thioacidolysis. In *Methods in Lignin Chemistry*; Lin, S. Y., Dence, C. W., Eds.; Springer-Verlag: Berlin, Germany, 1992; pp 334−349.

(17) Gellerstedt, G. Gel Permeation Chromatography. In *Methods in Lignin Chemistry*; Lin, S. Y., Dence, C. W., Eds.; Springer-Verlag: Berlin, Germany, 1992; pp 487−497.

(18) Li, J.; Gellerstedt, G.; Toven, K. Steam explosion lignins; their extraction, structure and potential as feedstock for biodiesel and chemicals. *Bioresour. Technol*. **2009**, *100*, 2556–2561.

(19) Caridad, R.; Ligero, P.; Vega, A.; Bao, M. Formic acid delignification of *Miscanthus sinensis*. *Cell. Chem. Technol*. **2004**, *38*, 235–244.

(20) Ligero, P.; Vega, A.; Bao, M. Acetosolv delignification of *Miscanthus sinensis* bark. Influence of process variables. *Ind. Crops Prod* **2005**, *21*, 235–240.

(21) Björkman, A. Studies on finely divided wood. Part I. Extraction of lignin with neutral solvents. *Sven. Papperstidn* **1956**, *13*, 477–485.

(22) Ralph, S. A.; Ralph, J.; Landucci, L. NMR Database of Lignin and Cell Wall Model Compounds, **2004**; U.S. Forest Products Laboratory, Madison, WI. (http://ars.usda.gov/Services/docs.htm?docid = 10491) (accesed July 2006).

(23) del Río, J. C.; Marques, G.; Rencoret, J.; Martínez, A. T.; Gutiérrez, A. Occurrence of naturally acetylated lignin units. *J. Agric. Food Chem*. **2007**, *55*, 5461–5468.

(24) Sun, R. C.; Fang, J. M.; Goodwin, A.; Lawther, J. M.; Bolton, J. Fractionation and characterization of ball-milled and enzyme lignins from abaca fibre. *J. Sci. Food Agric* **1999**, *79*, 1091–1098.

(25) del Río, J. C.; Gutiérrez, A. Chemical composition of abaca (*Musa textiles*) leaf fibers used for manufacturing of high quality paper pulps. *J. Agric. Food Chem*. **2006**, *54*, 4600–4610.

(26) Ralph, J. An unusual lignin from kenaf. *J. Nat. Prod*. **1996**, *59*, 341–342.

(27) Lu, F.; Ralph, J. Preliminary evidence for sinapyl acetate as a lignin monomer in kenaf. *Chem. Commun*. **2002**, 90–91.

(28) del Río, J. C.; Gutiérrez, A.; Martínez, A. T. Identifying acetylated lignin units in non-wood fibers using pyrolysis-gas chromatography/mass spectrometry. *Rapid Commun. Mass Spectrom*. **2004**, *18*, 1181–1185.

(29) Lu, F.; Ralph, J. Novel β-β structures in lignins incorporating acetylated monolignols. *Appita* **2005**, 233–237.

Received February 10, 2009. Revised manuscript received May 4, 2009. Accepted May 25, 2009. J.J.V. is grateful for the PGIDIT-INCITE fellowship from Xunta de Galicia to work in the Department of Fiber and Polymer Technology of the Royal Institute of Technology (KTH), which made this study possible.